Am J Physiol Regul Integr Comp Physiol 310: R55–R65, 2016.
First published November 15, 2015; doi:10.1152/ajpregu.00355.2015.

Adipogenic role of alternatively activated macrophages in β-adrenergic remodeling of white adipose tissue

Yun-Hee Lee,[1] Sang-Nam Kim,[1] Hyun-Jung Kwon,[1] Krishna Rao Maddipati,[2] and James G. Granneman[3]

[1]*College of Pharmacy, Yonsei University, Incheon, South Korea;* [2]*Lipidomics Core Facility and Department of Pathology, Wayne State University School of Medicine, Detroit, Michigan; and* [3]*Center for Integrative Metabolic and Endocrine Research, Wayne State University School of Medicine, Detroit, Michigan*

Submitted 13 August 2015; accepted in final form 21 October 2015

Lee YH, Kim S, Kwon H, Maddipati KR, Granneman JG. Adipogenic role of alternatively activated macrophages in β-adrenergic remodeling of white adipose tissue. *Am J Physiol Regul Integr Comp Physiol* 310: R55–R65, 2016. First published November 15, 2015; doi:10.1152/ajpregu.00355.2015.—De novo brown adipogenesis involves the proliferation and differentiation of progenitors, yet the mechanisms that guide these events in vivo are poorly understood. We previously demonstrated that treatment with a β_3-adrenergic receptor (ADRB3) agonist triggers brown/beige adipogenesis in gonadal white adipose tissue following adipocyte death and clearance by tissue macrophages. The close physical relationship between adipocyte progenitors and tissue macrophages suggested that the macrophages that clear dying adipocytes might generate proadipogenic factors. Flow cytometric analysis of macrophages from mice treated with CL 316,243 identified a subpopulation that contained elevated lipid and expressed CD44. Lipidomic analysis of fluorescence-activated cell sorting-isolated macrophages demonstrated that CD44+ macrophages contained four- to five-fold higher levels of the endogenous peroxisome-proliferator activated receptor gamma (PPARγ) ligands 9-hydroxyoctadecadienoic acid (HODE), and 13-HODE compared with CD44− macrophages. Gene expression profiling and immunohistochemistry demonstrated that ADRB3 agonist treatment upregulated expression of ALOX15, the lipoxygenase responsible for generating 9-HODE and 13-HODE. Using an in vitro model of adipocyte efferocytosis, we found that IL-4-primed tissue macrophages accumulated lipid from dying fat cells and upregulated expression of Alox15. Furthermore, treatment of differentiating adipocytes with 9-HODE and 13-HODE potentiated brown/beige adipogenesis. Collectively, these data indicate that noninflammatory removal of adipocyte remnants and coordinated generation of PPARγ ligands by M2 macrophages provides localized adipogenic signals to support de novo brown/beige adipogenesis.

adipose tissue macrophages; brown adipocytes; beige adipocytes; phagocytosis; adipogenesis

BROWN ADIPOSE TISSUE IS A specialized thermoregulatory organ that consumes lipid energy to generate heat, and the identification of brown adipose in adult humans has renewed interest in targeting the catabolic metabolism in brown adipose tissue to increase energy expenditure and improve metabolic profiles (18, 32, 40). Since the metabolic activity of human brown adipose tissue is typically low and varies greatly among individuals (23), an effort has been made to understand the mechanisms controlling brown fat mass and activity of brown adipocytes, particularly in nonclassical brown/beige adipocyte depots, such as in subcutaneous and visceral white adipose tissues. Although the specific mechanisms of induction of brown adipocyte phenotype in these locations remain controversial, in general, these include de novo brown adipogenesis from adipocyte progenitors and the induction of the brown adipocyte phenotype ("browning") in differentiated unilocular or paucilocular adipocytes (15, 28, 38).

To begin to address the mechanisms of de novo brown/beige adipogenesis in vivo, we developed a model in which brief infusion (3 days) of a β_3-adrenergic receptor (ADRB3) agonist recruits new multilocular UCP1$^+$ adipocytes (defined here as brown/beige adipocytes) from quiescent bipotential progenitors in gonadal white adipose tissue (gWAT) (14–16). In this model, CL316.243 (CL) treatment triggers the death of numerous unilocular white adipocytes, followed by clearance of the dead fat cells (efferocytosis) by resident macrophages that assume an M2 phenotype. Transgenic tracing and knockout experiments indicate that macrophage-derived chemokines, such as osteopontin, trigger the migration of adipocyte progenitors to the site of efferocytosis, where they proliferate and differentiate into new brown/beige adipocytes. The high degree of progenitor targeting to sites of efferocytosis strongly suggests that macrophages might act to create a niche that guides progenitor proliferation and differentiation. Our initial research focused on macrophage-derived chemokines and found that osteopontin is required for progenitor migration and proliferation. However, this proliferation is likely not sufficient to promote differentiation. Indeed, sustained progenitor proliferation induced by the activation of PDGFRα signaling causes pathogenic fibrosis (11, 25). Thus, we hypothesized that additional adipogenic signals, perhaps emanating locally from macrophages, might provide important signals that promote differentiation.

Here, extensive profiling by fluorescence-activated cell sorting (FACS) and gene expression analyses allowed us to identify and isolate a subpopulation of M2 macrophages that express the surface marker CD44 and participate in the catabolic remodeling of gWAT. Unbiased lipidomic analysis demonstrated that the CD44+ macrophages had an eicosanoid profile distinct from that of CD44− macrophages. Importantly, we detected the upregulation of several endogenous peroxisome-proliferator activate receptor gamma (PPARγ) ligands that are known to be arachidonate 15-lipoxygenase (Alox15) products. Consistent with the lipidomics data, macrophages found at sites of efferocytosis, the so-called "crown-like structures (CLS)", expressed high levels of Alox15 during CL treatment. In vitro coculture studies showed that dying adipocytes elevated IL-4-induced Alox15 and M2 marker expression in macrophages. Our in vitro experiments confirmed that the treatment with Alox15 products accelerated adipogenic differentiation of adipocyte progenitors. These results estab-

Address for reprint requests and other correspondence: J. G. Granneman, Center for Integrative Metabolic and Endocrine Research, Wayne State Univ. School of Medicine, Detroit, MI 48201 (e-mail: jgranne@med.wayne.edu).

lished an adipogenic role of the noninflammatory clearance of dying adipocytes and timely generation of PPARγ ligands by M2 macrophages in adipose tissue remodeling.

MATERIALS AND METHODS

Animals. All animal protocols were approved by the Institutional Animal Care and Use Committees at Wayne State University and Yonsei University. C57BL/6 mice (5–6 wk old, male) were purchased from the Jackson Laboratory (Bar Harbor, ME) and Orient Bio (Gyeonggi-Do, South Korea) and were fed a standard chow diet. For continuous ADRB3 stimulation, mice were infused with CL316,243 (Sigma, St. Louis, MO) (0.75 nmol/h) using osmotic pumps (Alzet, Cupertino, CA; 1007D) for up to 7 days.

Immunohistochemistry and immunocytochemistry. gWAT was processed for histological sections, and 5-μm-thick paraffin sections were subjected to immunohistochemical analysis, as previously described (15). For the immunochemical detection of 15-lipoxygenase (ALOX15) protein and lipids in macrophages, macrophages were cultured in four-chamber cell culture slides (SLP, Pocheon, Gyeonggi-do, South Korea), fixed with paraformaldehyde (4% in PBS), and subjected to immunocytochemical analysis, as previously described (5). The antibodies used for immunochemical detection were anti-15-lipoxygenase-1 antibody (mouse, 4 μg/ml; Abcam, Cambridge, MA) and anti-F4/80 antibody (rat, 1:100; AbD Serotec, Raleigh, NC). The secondary antibodies used were goat anti-mouse-Alexa Fluor 488 and goat anti-rat-Alexa Fluor 594 (1:500, Invitrogen, Molecular Probes, Carlsbad, CA). The omission of primary antibody was used as a negative control. DAPI (Sigma) was used for nuclear counterstaining.

Stromovascular cell fractionation and flow cytometry. Stromovascular cell (SVC) fractions were isolated from mouse gWAT, as previously described (15). Live cells or 4% paraformaldehyde (Electron Microscopy Science, Hatfield, PA)-fixed SVC were processed for cell surface marker staining using anti-F4/80 and anti-CD44 conjugated with-phycoerythrin (PE), FITC, or allophycocyanin (APC) (rat, 1:200, Biolegend, San Diego, CA). HCS LipidTOX Deep Red Neutral Lipid Stain H34477 (Invitrogen) was used for neutral lipid staining. 7-aminoactinomycin D (7-AAD; Biolegend), or DAPI (Sigma) were used to gate nucleated cells. Species-matched IgG (Biolegend) were used as nonspecific controls. Cell sorting and analytic cytometry were performed using BD FACS Vantage SE SORP and BD LSR II (BD Biosciences, San Jose, CA) flow cytometers, respectively. All compensation was performed using single color controls in BD FACS DiVa (BD Biosciences) software at the time of acquisition. Raw data were processed using FlowJo software (Tree Star, Ashland, OR). F4/80+ macrophages were isolated from SVC of gWAT of control mice and mice treated with CL using anti-F4/80-FITC (Biolegend) and anti-FITC microbeads (Miltenyi Biotech, San Diego, CA). PDGFRα+ cells were isolated from the SVC of white adipose tissue (WAT) of control mice using anti-PDGFRα-microbeads (Miltenyi Biotech).

Lipidomics analysis. FACS-isolated macrophages were homogenized by probe sonication on ice (3×10 s). The homogenates were supplemented with a mixture of internal standards (PGE_1-d_4, RvD_1-d_5, LTB_4-d_4, and 15-HETE-d_8, 5 ng each), extracted, and the lipid extracts were subjected to LC-MS-based lipidomic analysis to determine fatty acyl lipidome, according to the standard method described previously (21). Lipid extraction and liquid chromatography tandem-mass spectrometry (LC-MS/MS) analysis were performed at the Lipidomics Core Facility of the Pathology Department at Wayne State University.

Cell culture. PDGFRα+ cells isolated by magnetic cell sorting (MACS) from white adipose tissue of control mice were cultured to confluence in growth medium (DMEM; Welgene, Gyeongsan, Gyeongsangbukdo, South Korea) supplemented with 10% FBS (Gibco) and 1% penicillin/streptomycin (Gibco) at 37°C in a humidified atmosphere with 5% CO_2 and exposed to differentiation medium [DMEM supplemented with 10% FBS, 1% P/S, 2.5 mM isobutylmethylxanthine (IBMX, Cayman Chemical), 1 μM dexamethasone (Cayman Chemical), and 1 μg/ml insulin (Sigma)] or with the addition of 9-hydroxyoctadecadienoic acid (9-HODE; 68 μM/ml; Cayman Chemical, Ann Arbor, MI), 13-HODE (68 μM, Cayman Chemical), or rosiglitazone (Sigma, 20 nM) for 3 days.

C3H10T1/2 mouse embryonic fibroblasts (American Type Culture Collection, Manassas, VA) were cultured to confluence in growth medium and then exposed to bone morphogenetic protein 4 (20 ng/ml; R&D Systems, Minneapolis, MN) followed by exposure to differentiation medium for 3 days or with the addition of 9-HODE (68 μM, Cayman Chemical), 13-HODE (68 μM, Cayman Chemical), or rosiglitazone (Sigma, 20 nM) for 3 days. For long-term culture, cells were maintained in medium containing 1 μg/ml insulin for up to 10 days. To measure O_2 consumption rate of differentiated adipocytes, media were replaced with DMEM (phenol-red free) containing 10 μM isoproterenol or vehicle, and concentration of O_2 in media was monitored using Mito-ID Extracellular O_2 Sensor Probe (Enzo Life Sciences) at 37°C for 30 min. Fluorescence intensity vs. time was plotted and linear regression was applied to calculate the slope (O_2 consumption rate: dO_2/dT). To determine lipolysis of differentiated adipocytes, medium was replaced with fresh DMEM (phenol-red free) containing 10 μM isoproterenol or vehicle, and 4 h after isoproterenol treatment, the levels of glycerol released into the medium were determined using free glycerol reagent (Sigma).

MACS-isolated F4/80+ macrophages from gWAT were cultured at an initial concentration of 1×10^5 cells/ml in growth medium. For the coculture experiment, fully differentiated adipocytes obtained from the C3H10T1/2 cells (10 days postdifferentiation) were trypsinized and counted, and then 1×10^5 cells/ml were added to each well of 12-well dishes that contained macrophage cultures and incubated with vehicle or IL-4 (20 ng/ml; R&D Systems) for 2 days. For viability testing, 1×10^5 cells/well were seeded in 24-well plates and stained with a LIVE/DEAD viability/cytotoxicity kit (Invitrogen). For long-term imaging, differentiated C3H10T1/2 adipocytes were labeled with 4,4-difluoro-5-(2-thienyl)-4-bora-3a,4a-diaza-s-indacene-3-dodecanoic acid (BODIPY 558/568 C12) (Invitrogen Molecular Probes) and F4/80+ macrophages isolated from gWAT of control mice were labeled with Vybrant DiO Cell-Labeling Solution (Invitrogen Molecular Probes) overnight. BODIPY-labeled C3H10T1/2 cells were detached, added to the DiO-labeled macrophages, and then cocultured for 2 days with IL-4 (20 ng/ml). To monitor the phagocytosis of the dying adipocytes by the macrophages, live cell imaging was performed every 30 min with IncuCyte ZOOM live cell imaging equipment, (Essen Bioscience, Ann Arbor, MI), and the fluorescence intensity of the images was analyzed using IncuCyte ZOOM (Essen Bioscience) software.

Gene expression. RNA was extracted using TRIzol reagent (Invitrogen) and converted into cDNA by using high-capacity cDNA synthesis kit (Applied Biosystems, Waltham, MA). Quantitative real-time PCR was performed using SYBR Green Master Mix (Applied Biosystems) and ABI StepOne PLUS (Applied Biosystems) for 45 cycles, and the fold change for all the samples was calculated by the comparative cycle-threshold (Ct) method (i.e., $2-\Delta\Delta Ct$ method). Peptidylprolyl isomerase A was used as the housekeeping gene for mRNA expression analysis. cDNA was amplified using the following primers: Alox15 with 5′- GTGTCCCCCTGATGACTTGG-3′ (forward) and 5′-CATTCCCACCACGTACCGAT-3′ (reverse); cyclooxygenase 2 (COX2): prostaglandin-endoperoxide synthase 2 (Ptgs2) with 5′-CATCCCCTTCCTGCGAAGTT-3′ (forward) and 5′-CATGGGAGTTGGGCAGTCAT-3′ (reverse); fatty acid synthase (Fasn) with 5′-ACCTCTCCCAGGTGTGTGAC-3′ (forward) and 5′-CCTCCCGTACACTCACTCGT-3′ (reverse); hormone sensitive lipase (Lipe) with 5′- GCTGGGCTGTCAAGCACTGT-3′ (forward) and 5′-GTAACTGGGTAGGCTGCCAT-3′ (reverse). All other cDNAs were amplified using previously described primers (15).

Western blot analysis. Protein extracts were prepared, as previously described (17). Western blot analysis was performed using primary antibodies against 15-lipoxygenase-1 (mouse, Abcam) and β-actin (mouse, Santa Cruz Biotechnology, Dallas, TX) and secondary anti-mouse horseradish peroxidase antibodies (Cell Signaling Technology, Danvers, MA), as described previously (17). The blots were visualized with SuperSignal West Dura Substrate (Pierce-Invitrogen).

Statistical analysis. Statistical analyses were performed with GraphPad Prism 5 software (GraphPad Software, La Jolla, CA). Principal component analysis (PCA) was performed with XLStat software (Addinsoft, New York, NY) to detect the common variations between variables and to visualize clusters of correlated observations. Data are presented as means ± SE. Statistical significance between two groups was determined by unpaired *t*-test or Mann-Whitney *U*-test, as appropriate. Comparison among multiple groups was performed using a one-way ANOVA or two-way ANOVA, with Bonferroni post hoc tests to determine the relevant *P* values.

RESULTS

Isolation and characterization of lipid-laden macrophages from gWAT in CL-induced adipose tissue remodeling. We previously reported a model of de novo brown adipogenesis in which mature adipocytes that are killed by ADRB3 stimulation are replaced by localized clusters of new brown/beige adipocytes (14). Under these conditions, dead/dying adipocytes are cleared from the tissue by a network of noninflammatory M2 macrophages. To monitor the time course of the lipid metabolism of macrophages in gWAT remodeling, the lipid content in macrophages from gWAT was measured by flow cytometry at 3 to 7 days of CL treatment. As shown in Fig. 1, 3 days of CL treatment increased the number of F4/80+ macrophages, their lipid content, and granularity. This response was transient, as the number of macrophages and their lipid content returned to control levels by the 7th day of the CL treatment (Fig. 1, *A–C*). These data indicate rapid resolution of macrophage recruitment in ADRB3 remodeling of gWAT. Previous studies demonstrated that CD44 expression is strongly induced in macrophages that form CLS in adipose tissue (14). FACS analysis confirmed that expression of CD44 was closely correlated with lipid accumulation and, thus, could be used to isolate the subpopulation of lipid-laden macrophages (Fig. 1*D*).

Lipidomics analysis of isolated adipose tissue macrophages. We hypothesized that the metabolism of adipocyte-derived lipids by macrophages might be important in generating signals for localized differentiation of progenitors. To address this hypothesis, we performed LC-MS/MS lipidomic analysis of FACS-isolated CD44+ and CD44− macrophages from gWAT of CL-treated mice, as well as macrophages from untreated controls. Because bioactive oxygenated lipid mediators of arachidonic acids and other fatty acids are known to play an important role in immune responses and tissue remodeling (e.g., wound healing), eicosanomic profiling of macrophages was the main focus of this study (7, 30). The LC/MS/MS analysis of FACS-isolated CD44+ and CD44− macrophages detected a total of 91 lipid species, including cyclooxygenase (COX)-dependent, and lipoxygenase (LOX)-dependent pathway metabolites.

PCA showed that CD44+ macrophages had eicosanoid profiles distinct from those of CD44− macrophages (Fig. 2, *A* and *B*). CD44+ macrophages and CD44− macrophages were separated along the first component factor (F1) and the third component (F3) in PCA, which accounted for 67.1% and 12% of the overall variance, respectively (Fig. 2*A*). Interestingly, CD44− macrophages showed a lipid profile that was highly similar to that of the macrophages from the control conditions (Fig. 2*B*). F8, which accounts for only 0.3% of the variance, was able to segregate CD44− macrophages from the control conditions. PCA loading plot for the individual lipid classes identified major factors that account for the variance within the overall data set. 9-HODE and 13-HODE had the highest loading scores for F3, and the levels of these lipid species were significantly higher in the CD44+ macrophages compared with those in the CD44− macrophages and the macrophages from control conditions (Fig. 2*C*). 9-HODE and 13-HODE can be generated from linoleic acid (C18:2), an omega-6 fatty acid, via Alox15 pathway, and are known to be endogenous PPARγ ligands (8). In contrast to the levels of these Alox15 products,

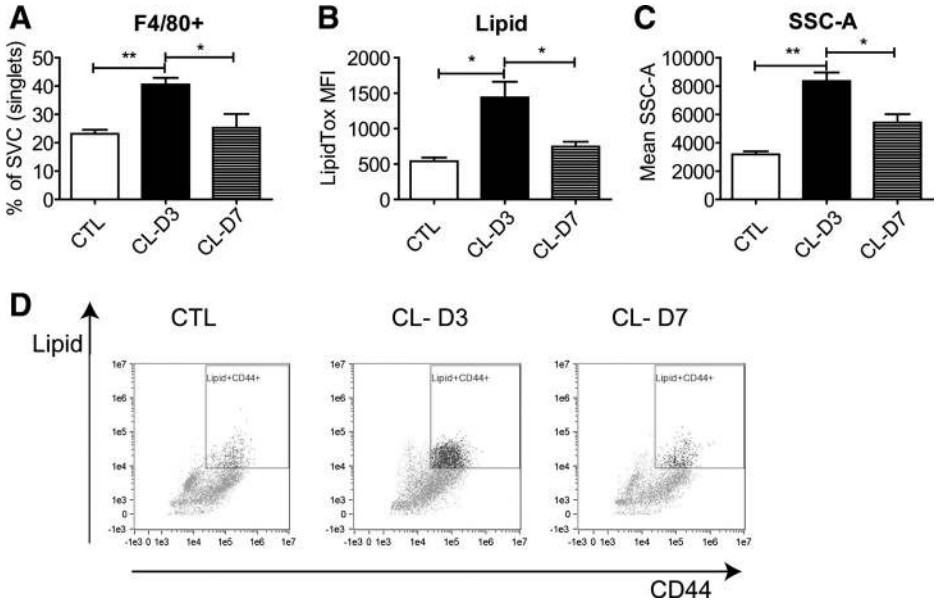

Fig. 1. Flow cytometric analysis of macrophages isolated from stromovascular cells (SVC) of gonadal white adipose tissue (gWAT) during β3 adrenergic receptor (ADRB3) activation. FACS analysis of the frequency (*A*), lipid staining intensity (mean fluorescence intensity: MFI) (*B*) and complexity (sidescatter area: SSA) (*C*) of macrophages in the gWAT of controls and mice treated with CL316,243 (CL) for up to 7 d. (means ± SE; $n = 3$ biological replicates of pooled tissue from two mice per condition; $^*P < 0.05$, $^{**}P < 0.01$). *D*: positive correlation between the CD44 expression and lipid accumulation in F4/80+ cells in the gWAT of control mice and mice treated with CL for up to 7 days ($P < 0.001$, $r^2 = 0.43$).

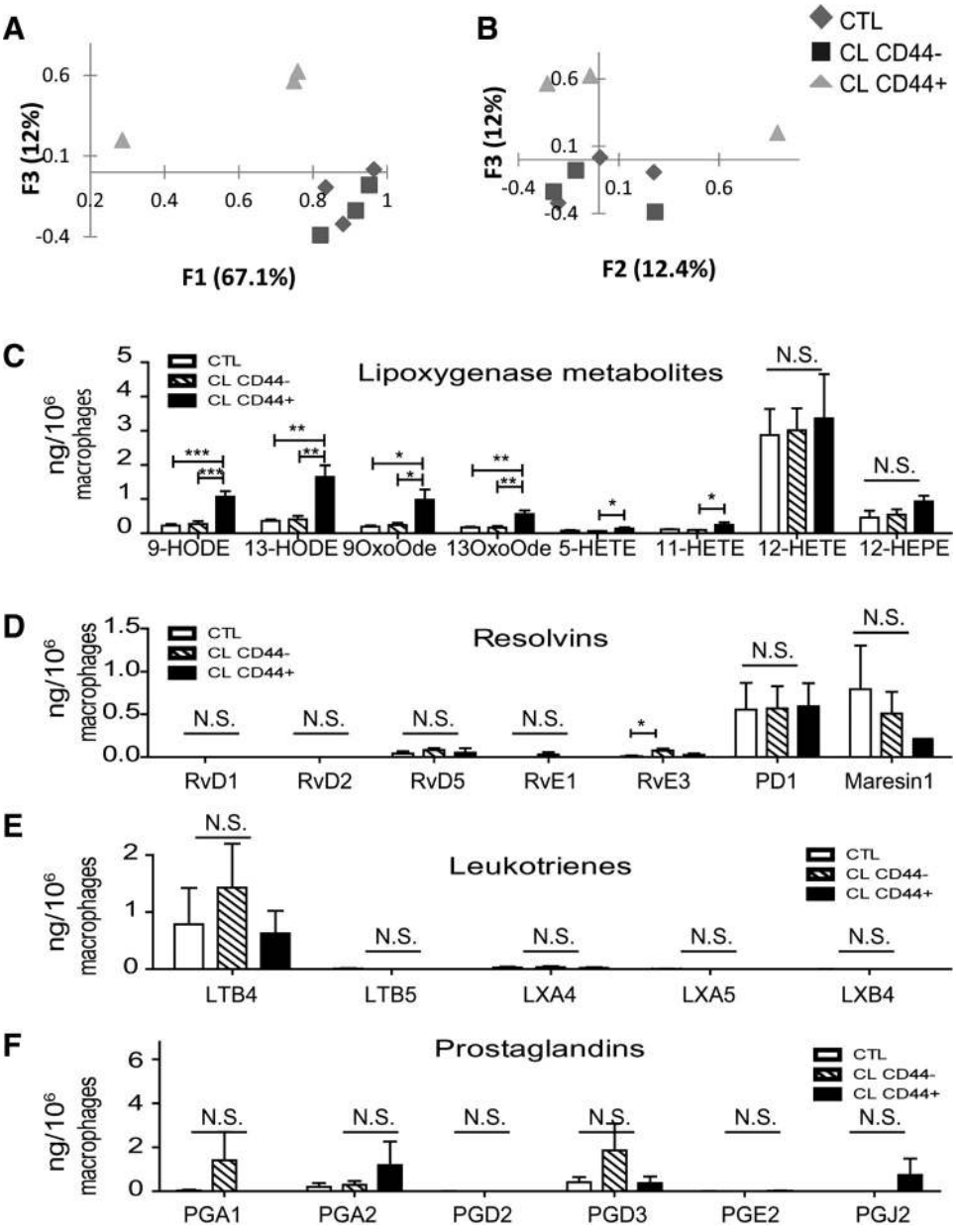

Fig. 2. Prostaglandin profiling of isolated macrophages from gWAT during ADRB3 stimulation. *A* and *B*: changes in the eicosanoids and derivatives in macrophages after CL treatment were measured by LC-MS/MS, and distinct characteristics were evaluated by PCA analysis. (CTL, control F4/80+; CL-CD44-, CL-d3 F4/80+CD44-; CL-CD44+, and CL-d3 F4/80+CD44+). *C–F*: levels of cyclooxygenase (COX)-dependent metabolites and lipoxygenase (LOX)-dependent metabolites, including prostaglandins, proresolving species, and leukotriene were plotted. *C*: ALOX15 products were significantly elevated in CD44+ macrophages compared with control conditions. Experiments were performed independently three times. Values are expressed as means ± SE of $n = 6$ (CTL), $n = 7$ (CL-CD44-), or $n = 5$ (CL-CD44+) biological replicates of pooled tissues from three mice. *P* values were calculated using the two-tailed unpaired *t*-test (*$P < 0.05$, **$P < 0.01$, ***$P < 0.001$; N.S., nonsignificant).

the levels of resolvins, leukotriene, and prostaglandins were not upregulated in CD44+ macrophages after CL treatment (Fig. 2, *D* and *F*), although these lipid species play an important role in the anti-inflammatory and proinflammatory responses of adipose tissue under various conditions (31). Resolvin 3E was slightly upregulated in CD44− macrophages (Fig. 2*D*).

Upregulation of Alox15 expression in CD44+ macrophages of gWAT after 3 days of CL treatment. Next, to determine the effect of CL treatment on lipid metabolism in macrophages, we performed gene expression profiling of CD44+F4/80+ and CD44− F4/80+ macrophages from the gWAT of mice treated with CL for 3 days, as well as F4/80+ macrophages from vehicle-treated controls (Fig. 3*A*). Quantitative PCR confirmed that CL treatment upregulated the levels of CD36 and Alox15 in the CD44+F4/80+ macrophages (Fig. 3*B*). However, CL treatment did not alter Cox2 expression (12). Consistent with mRNA analysis, immunohistochemical analysis demonstrated upregulation of ALOX15 protein expression in macrophages that form CLS at *day 3* of CL treatment (Fig. 3*C*).

Dying adipocytes potentiate IL-4-induced Alox15 expression in macrophages. To clarify the roles of macrophages in the removal of dying adipocytes, we further explored the interactions between dying adipocytes and macrophages using an in vitro coculture system. For this system, F4/80+ macrophages were isolated from gWAT by magnetic cell sorting (MACS) and maintained in growth medium. To induce adipocyte cell death, fully differentiated C3H10T1/2 adipocytes (10 days postdifferentiation) were trypsinized and replated. The adipocytes underwent gradual death with >98% cell death within 48 h after replating, as indicated by live/dead fluorescence staining and loss of adipocyte-specific gene expression (data not shown). We used this time point to examine interaction between dying adipocytes and macrophages.

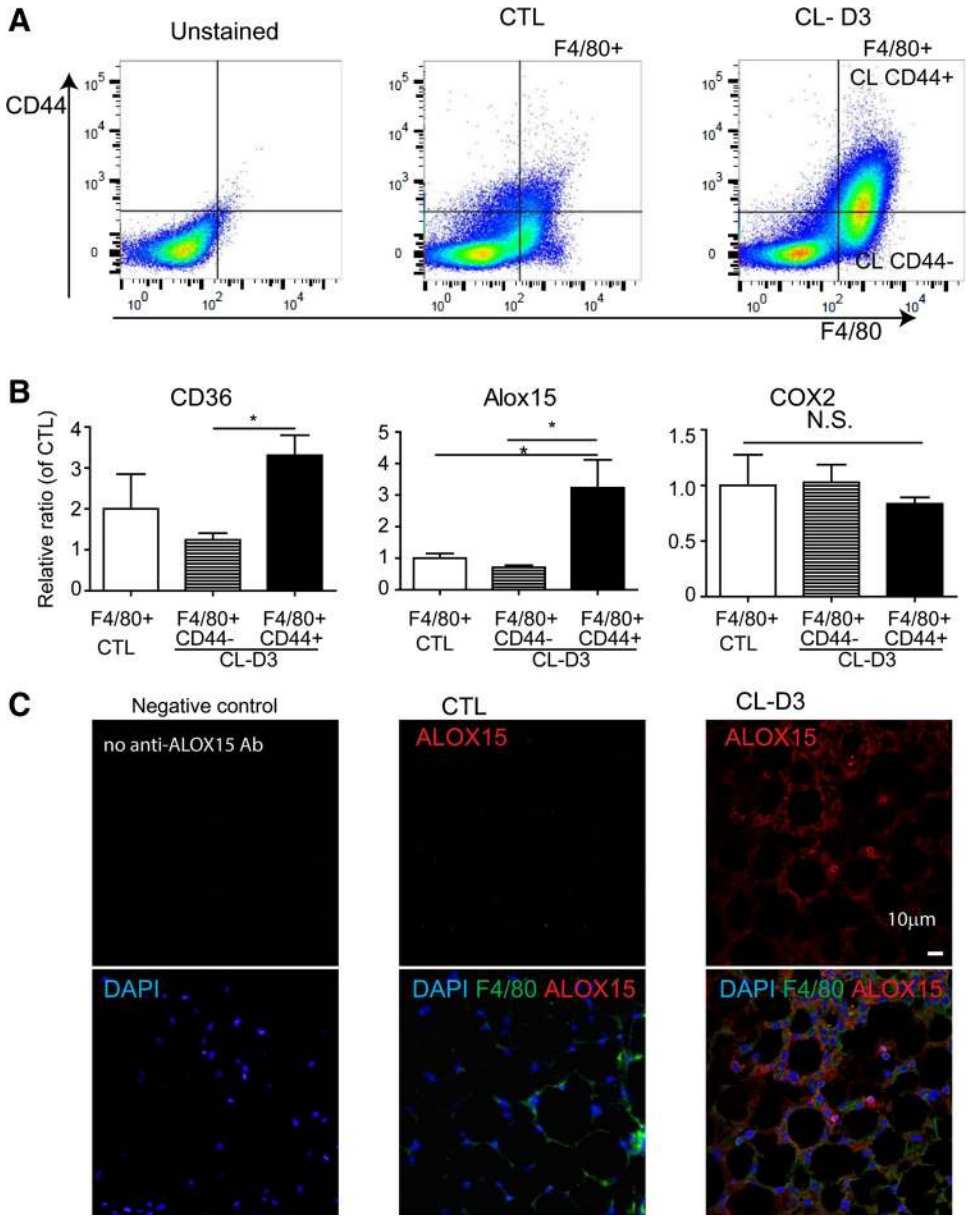

Fig. 3. Upregulation of Alox15 expression in CD44+ macrophages after 3 days of CL treatment. *A*: representative flow profiles indicate upregulation of CD44 expression after CL treatment. *B*: quantitative PCR of gene expression in FACS-isolated control- F4/80+, CL-CD44+, and CL-CD44- macrophages (means ± SE; $n = 3$ biological replicates of pooled tissues from 3 mice; $^*P < 0.05$). *C*: immunohistochemistry of 15-lipoxygenase (ALOX15) expression in F4/80+ macrophages in gWAT of mice treated with CL for 3 days. Nuclei were counterstained with DAPI.

To determine whether dying adipocytes affect macrophage polarization status, macrophages were cultured with dying adipocytes either in the presence or the absence of treatment with IL-4, which is a cytokine that is critical for inducing the M2 phenotype (34). Previous work demonstrated that ADRB3 stimulation upregulates IL-4 expression (14), and M2 polarization of macrophage is an important characteristic of ADRB3 remodeling of WAT. Dying adipocytes did not affect macrophage polarization in the absence of IL-4 (Fig. 4*A*). However, when IL-4 was present, the dying adipocytes significantly augmented expression of arginase 1 (Arg1) and Pparg (Fig. 4*A*). As expected, coculture with dying adipocyte did not affect the levels of proinflammatory marker expression (TNF-α, and IL-β1) in macrophages (Fig. 4*B*). These data imply that additional M2 stimuli are required for a synergistic anti-inflammatory interaction between the macrophages and dying adipocytes. Furthermore, coculture with dying adipocytes increased macrophage Alox15 expression, as determined by quantitative PCR (qPCR; Fig. 4*C*) and immunoblot analysis of ALOX15 protein levels (Fig. 4*D*).

The appearance of lipid-laden macrophages surrounding dead adipocytes in the ADRB3 remodeling of WAT suggested that M2 macrophages phagocytose dying adipocytes. To visualize the potential trafficking of lipids between macrophages and dying adipocytes, we utilized the coculture system described above. Adipocyte lipids were labeled with the fluorescent fatty acid analog BODIPY-C12, while macrophages were labeled with the fluorescent cell tracer DiO. Long-term imaging demonstrated loss of adipocyte-associated BODIPY label, implying that the dying adipocytes underwent phagocytosis by macrophages (Fig. 5*A*). Concurrently, the formation of BODIPY-positive lipid droplets and expression of ALOX15 protein in macrophages were observed [83.7 ± 3.0% of BODIPY+ cells were ALOX15 positive ($n = 3$; means ± SE)] (Fig. 5, *B* and *C*). Collectively, these data suggest that the noninflammatory clearance of dying adipocytes by M2

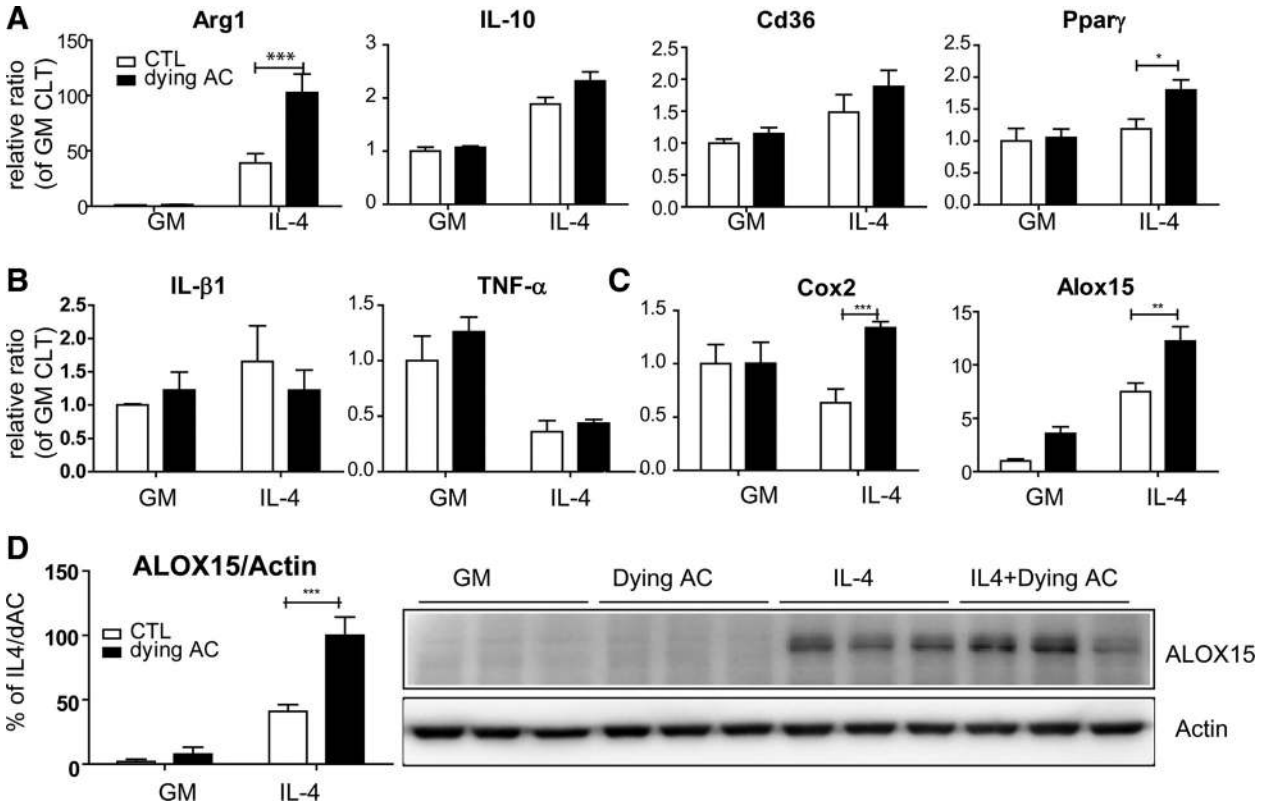

Fig. 4. In vitro coculture with dying adipocytes (AC) increase M2 macrophage marker expression and Alox15 expression in macrophages. Quantitative PCR of M2 macrophage marker (*A*), M1 marker (*B*), and lipid oxygenase (*C*) expression in F4/80+ macrophages cocultured with dying adipocytes in growth medium (GM) with or without IL-4 (means ± SE; $n = 6$ biological replicates from two independent experiments; $^*P < 0.05$, $^{**}P < 0.01$, $^{***}P < 0.001$). *D*: Immunoblot analysis of ALOX15 protein expression in macrophages cocultured with dying adipocytes with or without IL-4. A representative immunoblot out of 3 independent experiments is shown. Values are expressed as means ± SE; $n = 9$ biological replicates per condition from three independent experiments; $^{***}P < 0.001$.

macrophages involves offloading of the adipocyte lipids to macrophages, potentiation of M2 polarization, and upregulation of ALOX15 protein expression. Consistent with the gene expression profiling analysis of macrophages obtained from the adipose tissue of CL-treated mice, coculture with dying adipocytes increased the CD44 expression in the macrophages, as measured by qPCR (Fig. 5*D*) and flow cytometry (Fig. 5, *E* and *F*). In addition, FACS analysis demonstrated that coculture with dying adipocytes upregulates the ALOX15 protein expression in the CD44+ macrophages (Fig. 5, *E* and *F*).

The ALOX15 products 9-HODE and 13-HODE potentiate in vitro brown/beige adipogenesis from progenitors. Alox15 catalytic products, 9-HODE and 13-HODE, can exert diverse physiological effects by activating surface and nuclear receptors that include TRPV1, GPR132, and PPARγ. PPARγ is a master regulator of adipogenesis, and the interaction of Alox15 products with PPARγ in other cell types (9) suggested that these lipid mediators might promote differentiation of adipocyte progenitors. To address this question, we isolated PDGFRα+ adipocyte progenitors from mouse WAT using MACS and exposed confluent progenitors to a standard adipogenic cocktail containing vehicle, 9-HODE, or 13-HODE. Rosiglitazone, a potent synthetic PPARγ agonist, was used as the positive control. Alox15 products induced a twofold increase in adipogenic differentiation of the progenitors, as measured by lipid (BODIPY) staining (Fig. 6, *A* and *B*). This enhancement was comparable to that produced by rosiglitazone treatment. Consistent with the effects on lipid accumulation and morphological changes, 9-HODE and 13-HODE treatment modestly potentiated expression of general adipocyte markers fatty acid synthase (Fasn), and hormone-sensitive (Lipe), and adipose triglyceride lipase (Pnpla2), but did not affect expression of Pparg (Fig. 6*C*). More strikingly, 9-HODE and 13-HODE strongly potentiated expression of brown adipocyte markers, including elongation of very long-chain fatty acids like 3 (Elovl3) and cell death-inducing DNA fragmentation factor alpha-like effector A (Cidea), as well as genes involved in mitochondrial biogenesis and fatty acid oxidation [cytochrome *c* oxidase subunit VIIIb (Cox8b), and acyl-coenzyme A dehydrogenase, medium chain (Acadm)]. Importantly, 9-HODE and 13-HODE potentiated the induction of uncoupling protein 1 (Ucp1) expression by isoproterenol by two- to three-fold (Fig. 6*D*). Consistent with the observed pattern of gene expression, PDGFRα+ cells differentiated in the presence of 9-HODE and 13-HODE hydrolyzed more triglyceride (Fig. 6*E*) and consumed more oxygen (Fig. 6*F*) in response to stimulation by isoproterenol. While not shown, similar results were obtained with the C3H10T1/2 cell line.

DISCUSSION

Adipose tissue renewal and plasticity are central to long-term metabolic health, yet the mechanisms that guide these

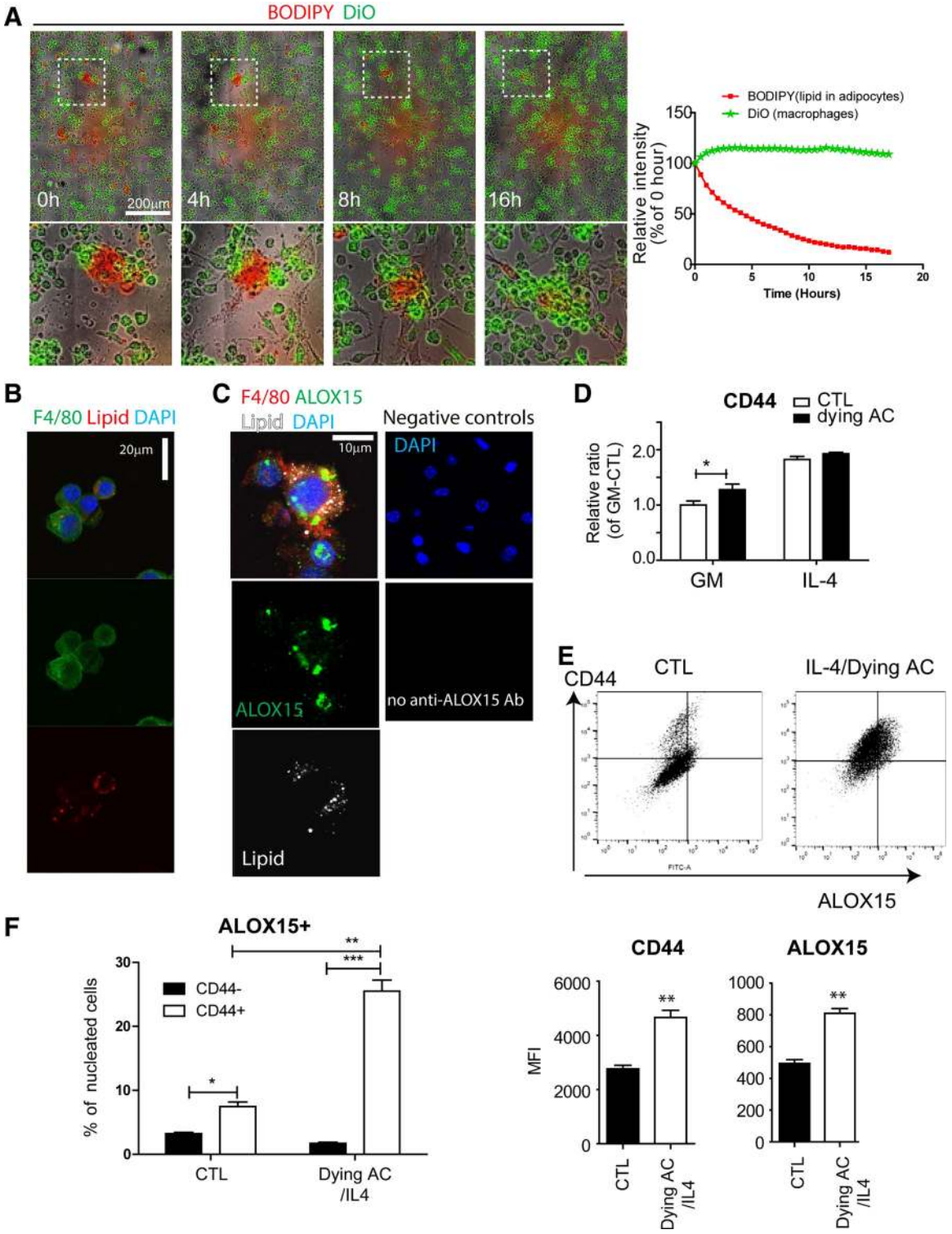

Fig. 5. M2 macrophages phagocytose dying ACs. *A*: long-term live imaging of macrophages cocultured with dying ACs. Macrophages were stained with DiO (green) for long-term tracing, and adipocytes were labeled with C12-BODIPY (red) separately. Images are representative of three independent experiments. *B*: lipid detection in macrophages cocultured with dying adipocytes. *C*: immunostaining indicates ALOX15 expression in lipid+ macrophages cocultured with dying adipocytes. Nuclei were counterstained with DAPI. *D*: quantitative PCR analysis of CD44 mRNA expression in F4/80+ macrophages cocultured with dying adipocytes. *E* and *F*: FACS analysis of CD44 and ALOX15 expression in macrophages cocultured with dying adipocytes and IL-4 treatment. CTL, control. *P* values were calculated using the two-tailed unpaired *t*-test (means ± SE; $n = 3$ per condition; $^{*}P < 0.05$, $^{**}P < 0.01$, $^{***}P < 0.001$).

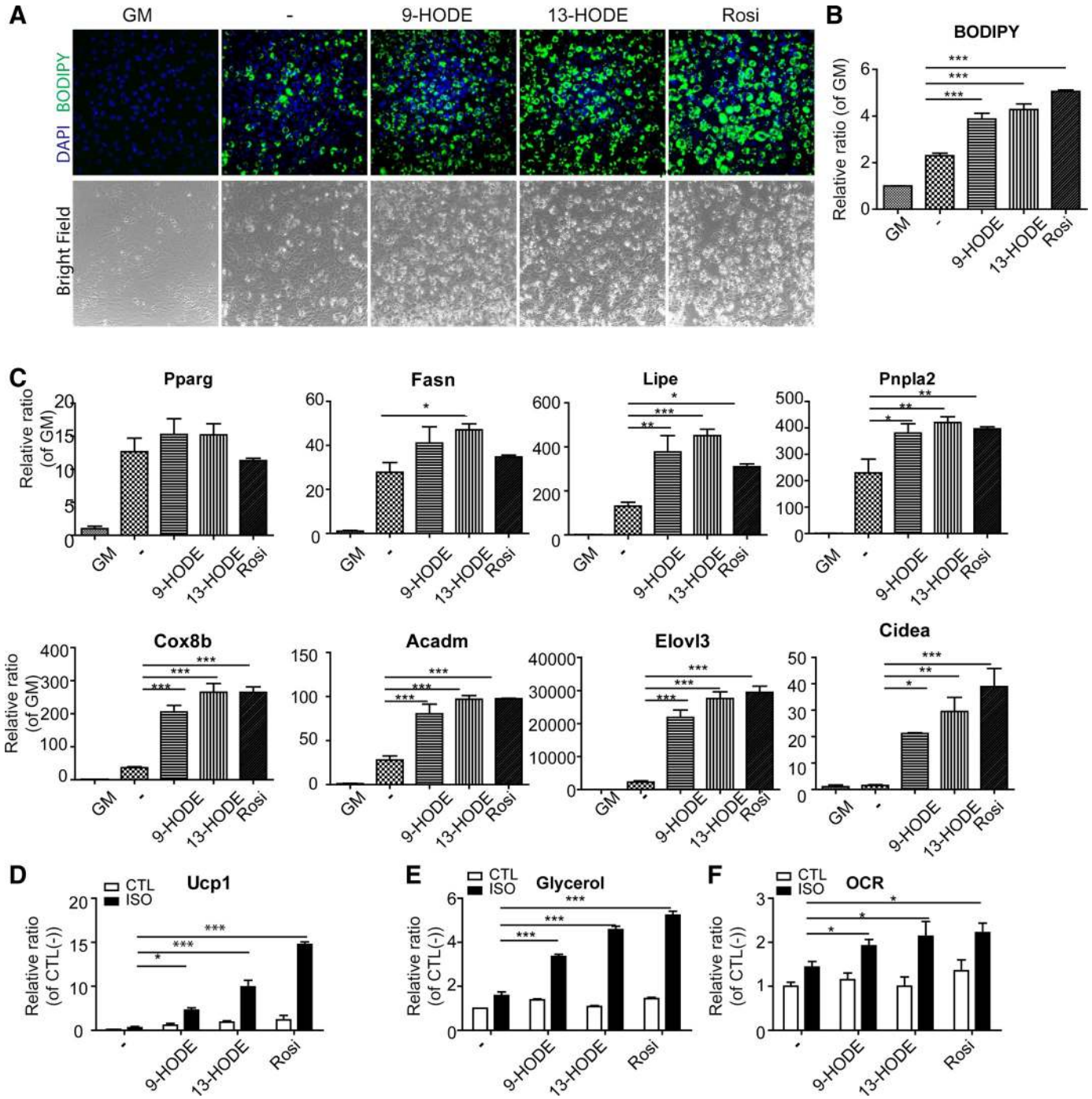

Fig. 6. In vitro effect of 9-hydroxyoctadecadienoic acid (9-HODE) and 13-HODE on brown/beige adipogenic differentiation of adipocyte progenitors. PDGFRα+ progenitors from WAT (*A–F*) were differentiated under standard adipogenic condition or with the addition of 9-HODE (68 μM), 13-HODE (68 μM), or rosiglitazone (20 nM) for 3 days. *A*: lipid accumulation was detected by BODIPY staining and nuclei were counterstained with DAPI. *B*: quantification of BODIPY fluorescent intensity ($n = 3$ per condition). *C*: quantitative PCR analysis of adipocyte gene expression ($n = 3$ per condition). Quantitative PCR analysis of UCP1 induction ($n = 3$ per condition) (*D*) and glycerol levels in media under control conditions or 4 h after isoproterenol (10 μM) treatment ($n = 3$ per condition) (*E*). Oxygen consumption rate (OCR) in the absence and presence of 10 μM isoproterenol ($n = 4$ per condition). *P* values were calculated using the two-tailed unpaired *t*-test (means ± SE; $*P < 0.05$, $**P < 0.01$, $***P < 0.001$).

processes in vivo are poorly understood (13). We previously reported that remodeling of gWAT induced by ADRB3 stimulation is associated with evidence of tissue restoration, including death of adipocytes, recruitment of anti-inflammatory macrophages, and proliferation/differentiation of progenitors (14). This work suggests that macrophages that clear dead fat cells create a localized adipogenic niche where progenitors proliferate and differentiate. Although our previous work identified osteopontin from macrophages as a chemotactic factor that recruits PDGFRα+ progenitors, the factors that induce adipogenesis remained unknown. In the current study, we attempted to deconstruct brown/beige

adipogenic niches by analyzing the lipid-laden macrophages that were actively clearing dying adipocytes. Our results confirm that the surface marker CD44 defines the subpopulation of M2-polarized macrophages that clear fat cells and metabolize the subsequent lipid remains. Lipidomic analysis of the CD44+ macrophages demonstrated a distinct fatty acyl lipidomic profile containing high levels of 13-HODE and 9-HODE, which are generated by Alox15 activity. Consistent with this, we found that in vivo CL treatment upregulated Alox15 mRNA expression levels in FACS-isolated CD44+ macrophages from gWAT and elevated ALOX15 protein levels in the macrophages that form crown-like structures.

We created an in vitro model of fat cell phagocytosis that replicated several important aspects of fat cell clearance in vivo. Dead fat cells alone provided minimal macrophage activation. However, treatment of cultures with IL-4, which increases during CL treatment (14), upregulated M2 marker expression (Arg1) and downregulated TNF-α, proinflammatory cytokine. Interestingly, the presence of dead fat cells enhanced expression of Alox15 and Pparg in a fashion that would increase uptake of lipid, amplify PPARγ-mediated signaling, and enhance the M2 phenotype. Recent research indicates that the clearance of apoptotic cells by resident macrophages requires Alox15-mediated oxidation of phosphatidylethanolamine, which inhibits uptake of apoptotic cells by inflammatory monocytes (33). Although the precise molecular mechanisms of noninflammatory adipocyte removal are largely unknown, we anticipate that further development of the in vitro model described here might be useful for addressing these questions.

The products of Alox15, 9-HODE, and 13-HODE are known PPARγ ligands (9, 24), and Alox15 activity is required in the early phase of in vitro adipogenesis (22). In the present experiments, we found that 9-HODE and 13-HODE promoted the adipogenic differentiation of PDGFRα+ progenitors, and strongly upregulated markers of brown/beige adipocytes, including UCP1 and genes involved in mitochondrial fatty acid oxidation. Functionally, PDGFRα+ progenitors that were differentiated in the presence of 9-HODE and 13-HODE were more responsive to the adrenergic induction of UCP1, and the concurrent stimulation of lipolysis and oxidative metabolism. These data are consistent with previous reports showing that PPARγ agonist promote brown/beige adipogenic differentiation of white adipocytes (26, 27) and suggest that local exposure to macrophage-derived PPARγ ligands directs bipotential progenitors toward a brown adipocyte phenotype. We note that neither 9-HODE nor 13-HODE without adipogenic cocktail (insulin, IBMX, dexamethasone) was able to induce adipogenic differentiation of progenitors, suggesting additional adipogenic signals, such as activation of the cAMP pathway, might be required.

In addition to the generation of PPARγ ligands, ALOX15 catalytic activity regulates anti-inflammatory and proinflammatory pathways. In particular, several pathologic conditions have been shown to correlate with proinflammatory lipoxygenase pathways (5). For example, upregulation of 12/15-lipoxygenase in visceral adipose tissue is implicated in the development of insulin resistance and obesity-related metabolic disease. In this pathologic condition, the levels of 12-hydroxyeicosatetraenoic acid (HETE), an Alox15 product resulting from arachidonic acid oxidation, are correlated with proinflammatory cytokine expression and the pathogenesis of insulin resistance (19). Genetic deletion of Alox15 expression in a mouse model has been shown to be protective against diet-induced obesity-related metabolic abnormalities (6, 29). In our study, the levels of proinflammatory products (e.g., 12-HETE) (2, 3) did not change in the macrophages from WAT that underwent β-adrenergic remodeling. Alox15 is also involved in the generation and metabolism of proresolving lipid species (31).

Previous work demonstrated that Alox15 products promote the CD36-mediated uptake of oxidized low-density lipoprotein (oxLDL), contributing to the generation of foam cells and the pathogenesis of atherosclerosis (24). It is important to note that lipid accumulation in macrophages is transient in CL-induced adipose tissue remodeling, whereas CLS macrophages in the obese conditions can become enduring foam cells (4). CLS macrophages recruited by high-fat-diet feeding have been reported to manifest proinflammatory M1 phenotypes (20) or M1/M2 mixed phenotype (39). We speculate that the disposal or rapid consumption of lipid in macrophages is a key factor that prevents the inflammatory stimulation of phagocytes. However, it remains to be determined how the engulfed lipids can be processed rapidly, escaping from potential inflammatory responses. Possibly, adipose tissue macrophages in metabolically healthy adipose tissue have a higher capacity to process or mobilize lipids, including elevated lipolytic activity (10), mitochondrial β-oxidation, and lysosomal degradation (39). Additionally, progenitors may use lipid from macrophages to accelerate concurrent de novo adipogenesis. Interestingly, the presence of dying adipocytes enhanced M2 marker and Alox15 expression. Because the Alox15 enzyme oxygenates polyunsaturated fatty acids and phospholipids of biological membranes, dying adipocytes may provide substrates for 9-HODE and 13-HODE production. It remains to be determined whether membrane linoleic acid, or hydrolytic products from adipocyte triglycerides can be used as a source of PPARγ ligand production in macrophages.

Perspectives and Significance

While much progress has been made regarding the transcriptional mechanisms that guide adipogenesis in vitro, how and where adipogenesis occur in vivo is poorly understood (13, 38). Growing evidence indicates that adipogenesis in vivo involves highly localized interactions within a defined tissue niche and that such interactions are critically important for precise, noninflammatory tissue remodeling and repair. The present study emphasizes pivotal roles of lipid metabolism carried out by macrophages in the noninflammatory removal of dying adipocytes and de novo brown/beige adipogenesis. Moreover, our results demonstrate that the cellular elements of these adipogenic niches can be isolated and modeled in vitro, allowing greater mechanistic analysis of niche interactions. An understanding of adipogenic niches under pathological and therapeutic conditions may lead to development of novel treatments to produce beneficial adipocyte phenotypes and, thereby, prevent or reverse obesity-related diseases.

ACKNOWLEDGMENTS

This research was supported by National Institutes of Health grants DK62292 and DK76629 (JGG), by National Research Foundation of Korea grant NRF-2014R1A6A3A04056472 (YHL), Yonsei Research Fund (2015), and by Korea Mouse Phenotyping Project (2013M3A9D5072550) of the Ministry of Science, ICT and Future Planning through the National Research Foundation (YHL). Support for lipidomics analysis was provided by the National Center for Research Resources, National Institutes of Health Grant S10RR027926.

DISCLOSURES

No conflicts of interest, financial or otherwise, are declared by the authors.

AUTHOR CONTRIBUTIONS

Author contributions: Y.-H.L. and J.G.G. conception and design of research; Y.-H.L., S.-N.K., and H.-J.K. performed experiments; Y.-H.L., S.-N.K., H.-J.K., K.R.M., and J.G.G. analyzed data; Y.-H.L., K.R.M., and J.G.G. interpreted results of experiments; Y.-H.L. and H.-J.K. prepared figures; Y.-H.L. and J.G.G. drafted manuscript; Y.-H.L., K.R.M., and J.G.G. edited and revised manuscript; J.G.G. approved final version of manuscript.

REFERENCES

1. **Alsalem M, Wong A, Millns P, Arya PH, Chan MS, Bennett A, Barrett DA, Chapman V, Kendall DA.** The contribution of the endogenous TRPV1 ligands 9-HODE and 13-HODE to nociceptive processing and their role in peripheral inflammatory pain mechanisms. *Br J Pharmacol* 168: 1961–1974, 2013.
2. **Chakrabarti SK, Cole BK, Wen Y, Keller SR, Nadler JL.** 12/15-lipoxygenase products induce inflammation and impair insulin signaling in 3T3–L1 adipocytes. *Obesity (Silver Spring)* 17: 1657–1663, 2009.
3. **Chakrabarti SK, Wen Y, Dobrian AD, Cole BK, Ma Q, Pei H, Williams MD, Bevard MH, Vandenhoff GE, Keller SR, Gu J, Nadler JL.** Evidence for activation of inflammatory lipoxygenase pathways in visceral adipose tissue of obese Zucker rats. *Am J Physiol Endocrinol Metab* 300: E175–E187, 2011.
4. **Cinti S, Mitchell G, Barbatelli G, Murano I, Ceresi E, Faloia E, Wang S, Fortier M, Greenberg AS, Obin MS.** Adipocyte death defines macrophage localization and function in adipose tissue of obese mice and humans. *J Lipid Res* 46: 2347–2355, 2005.
5. **Cole BK, Lieb DC, Dobrian AD, Nadler JL.** 12- and 15-lipoxygenases in adipose tissue inflammation. *Prostaglandins Other Lipid Mediat* 104–105: 84–92, 2013
6. **Cole BK, Morris MA, Grzesik WJ, Leone KA, Nadler JL.** Adipose tissue-specific deletion of 12/15-lipoxygenase protects mice from the consequences of a high-fat diet. *Mediators Inflamm* 2012: 851798, 2012.
7. **Haeggstrom JZ, Funk CD.** Lipoxygenase and leukotriene pathways: biochemistry, biology, and roles in disease. *Chem Rev* 111: 5866–5898, 2011.
8. **Harmon GS, Lam MT, Glass CK.** PPARs and lipid ligands in inflammation and metabolism. *Chem Rev* 111: 6321–6340, 2011.
9. **Huang JT, Welch JS, Ricote M, Binder CJ, Willson TM, Kelly C, Witztum JL, Funk CD, Conrad D, Glass CK.** Interleukin-4-dependent production of PPAR-γ ligands in macrophages by 12/15-lipoxygenase. *Nature* 400: 378–382, 1999.
10. **Huang SC, Everts B, Ivanova Y, O'Sullivan D, Nascimento M, Smith AM, Beatty W, Love-Gregory L, Lam WY, O'Neill CM, Yan C, Du H, Abumrad NA, Urban JF Jr, Artyomov MN, Pearce EL, Pearce EJ.** Cell-intrinsic lysosomal lipolysis is essential for alternative activation of macrophages. *Nat Immunol* 15: 846–855, 2014.
11. **Iwayama T, Steele C, Yao L, Dozmorov MG, Karamichos D, Wren JD, Olson LE.** PDGFRα signaling drives adipose tissue fibrosis by targeting progenitor cell plasticity. *Genes Dev* 29: 1106–1119, 2015.
12. **Kuhn H, Thiele BJ.** The diversity of the lipoxygenase family: Many sequence data but little information on biological significance1. *FEBS Lett* 449: 7–11, 1999.
13. **Lee YH, Mottillo EP, Granneman JG.** Adipose tissue plasticity from WAT to BAT and in between. *Biochim Biophys Acta* 1842: 358–369, 2014.
14. **Lee YH, Petkova Anelia P, and Granneman JG.** Identification of an adipogenic niche for adipose tissue remodeling and restoration. *Cell Metab* 18: 355–367, 2013.
15. **Lee YH, Petkova Anelia P, Mottillo Emilio P, Granneman JG.** In vivo identification of bipotential adipocyte progenitors recruited by β_3-adrenoceptor activation and high-fat feeding. *Cell Metab* 15: 480–491, 2012.
16. **Lee YH, Thacker RI, Hall BE, Kong R, Granneman JG.** Exploring the activated adipogenic niche: Interactions of macrophages and adipocyte progenitors. *Cell Cycle* 13: 184–190, 2014.
17. **Lee YH, Petkova AP, Konkar AA, Granneman JG.** Cellular origins of cold-induced brown adipocytes in adult mice. *FASEB J* 29: 286–299, 2015.
18. **Lidell ME, Enerback S.** Brown adipose tissue—a new role in humans? *Nat Rev Endocrinol* 6: 319–325, 2010.
19. **Lieb DC, Brotman JJ, Hatcher MA, Aye MS, Cole BK, Haynes BA, Wohlgemuth SD, Fontana MA, Beydoun H, Nadler JL, Dobrian AD.** Adipose tissue 12/15 lipoxygenase pathway in human obesity and diabetes. *J Clin Endocrinol Metab* 99: E1713–E1720, 2014.
20. **Lumeng CN, Bodzin JL, Saltiel AR.** Obesity induces a phenotypic switch in adipose tissue macrophage polarization. *J Clin Invest* 117: 175–184, 2007.
21. **Maddipati KR, Romero R, Chaiworapongsa T, Zhou SL, Xu Z, Tarca AL, Kusanovic JP, Munoz H, Honn KV.** Eicosanomic profiling reveals dominance of the epoxygenase pathway in human amniotic fluid at term in spontaneous labor. *FASEB J* 28: 4835–4846, 2014.
22. **Madsen L, Petersen RK, Sorensen MB, Jorgensen C, Hallenborg P, Pridal L, Fleckner J, Amri EZ, Krieg P, Furstenberger G, Berge RK, Kristiansen K.** Adipocyte differentiation of 3T3–L1 preadipocytes is dependent on lipoxygenase activity during the initial stages of the differentiation process. *Biochem J* 375: 539–549, 2003.
23. **Muzik O, Mangner TJ, Granneman JG.** Assessment of oxidative metabolism in brown fat using PET imaging. *Front Endocrinol* 3: 2012.
24. **Nagy L, Tontonoz P, Alvarez JGA, Chen H, Evans RM.** Oxidized LDL regulates macrophage gene expression through ligand activation of PPARγ. *Cell* 93: 229–240, 1998.
25. **Olson LE, Soriano P.** Increased PDGFRα activation disrupts connective tissue development and drives systemic fibrosis. *Dev Cell* 16: 303–313, 2009.
26. **Petrovic N, Shabalina IG, Timmons JA, Cannon B, Nedergaard J.** Thermogenically competent nonadrenergic recruitment in brown preadipocytes by a PPARγ agonist. *Am J Physiol Endocrinol Metab* 295: E287–E296, 2008.
27. **Petrovic N, Walden TB, Shabalina IG, Timmons JA, Cannon B, Nedergaard J.** Chronic peroxisome proliferator-activated receptor γ (PPARγ) activation of epididymally derived white adipocyte cultures reveals a population of thermogenically competent, UCP1-containing adipocytes molecularly distinct from classic brown adipocytes. *J Biol Chem* 285: 7153–7164, 2010.
28. **Rosenwald M, Perdikari A, Rülicke T, Wolfrum C.** Bi-directional interconversion of brite and white adipocytes. *Nat Cell Biol* 15: 659–667, 2013.
29. **Sears DD, Miles PD, Chapman J, Ofrecio JM, Almazan F, Thapar D, Miller YI.** 12/15-lipoxygenase is required for the early onset of high fat diet-induced adipose tissue inflammation and insulin resistance in mice. *PLoS One* 4: e7250, 2009.
30. **Serhan CN, Petasis NA.** Resolvins and protectins in inflammation resolution. *Chem Rev* 111: 5922–5943, 2011.
31. **Spite M, Clària J, Serhan CN.** Resolvins, Specialized Proresolving Lipid Mediators, and Their Potential Roles in Metabolic Diseases. *Cell Metab* 19: 21–36, 2014.
32. **Stanford KI, Middelbeek RJW, Townsend KL, An D, Nygaard EB, Hitchcox KM, Markan KR, Nakano K, Hirshman MF, Tseng YH, Goodyear LJ.** Brown adipose tissue regulates glucose homeostasis and insulin sensitivity. *J Clin Invest* 123: 215–223, 2013.
33. **Uderhardt S, Herrmann M, Oskolkova Olga V, Aschermann S, Bicker W, Ipseiz N, Sarter K, Frey B, Rothe T, Voll R, Nimmerjahn F, Bochkov Valery N, Schett G, Krönke G.** 12/15-Lipoxygenase orchestrates the clearance of apoptotic cells and maintains immunologic tolerance. *Immunity* 36: 834–846, 2012.
34. **Van Dyken SJ, Locksley RM.** Interleukin-4- and interleukin-13-mediated alternatively activated macrophages: roles in homeostasis and disease. *Ann Rev Immunol* 31: 317–343, 2013.
35. **Vangaveti V, Baune BT, Kennedy RL.** Hydroxyoctadecadienoic acids: novel regulators of macrophage differentiation and atherogenesis. *Ther Adv Endocrinol Metab* 1: 51–60, 2010.
36. **Vangaveti VN, Shashidhar VM, Rush C, Malabu UH, Rasalam RR, Collier F, Baune BT, Kennedy RL.** Hydroxyoctadecadienoic acids

regulate apoptosis in human THP-1 cells in a PPARγ-dependent manner. *Lipids* 49: 1181–1192, 2014.

37. **Wang L, Gill R, Pedersen TL, Higgins LJ, Newman JW, Rutledge JC.** Triglyceride-rich lipoprotein lipolysis releases neutral and oxidized FFAs that induce endothelial cell inflammation. *J Lipid Res* 50: 204–213, 2009.
38. **Wang QA, Tao C, Gupta RK, Scherer PE.** Tracking adipogenesis during white adipose tissue development, expansion and regeneration. *Nat Med* 19: 1338–1344, 2013.
39. **Xu X, Grijalva A, Skowronski A, van Eijk M, Serlie Mireille J, Ferrante Jr, Anthony W.** Obesity activates a program of lysosomal-dependent lipid metabolism in adipose tissue macrophages independently of classic activation. *Cell Metab* 18: 816–830, 2013.
40. **Yoneshiro T, Aita S, Matsushita M, Kayahara T, Kameya T, Kawai Y, Iwanaga T, Saito M.** Recruited brown adipose tissue as an antiobesity agent in humans. *J Clin Invest* 123: 3404–3408, 2013.